Analysis of melting in an enclosure under boundary condition of the third kind

Yuwen Zhang
Department of Mechanical Engineering
New Mexico State University
Las Cruces, NM 88003, USA

Abstract

Natural convection controlled melting in a rectangular enclosure with convective heating on one side was investigated analytically. The liquid phase can be divided into three regions: (1) cold boundary layer near solid-liquid interface, (2) warm boundary layer near the heated vertical wall, and (3) the core region between these two boundary layers. The governing equations in the three regions are nondimensionalized into a set of ordinary differential equations and solved numerically. The effect of Biot number on the wall and core temperatures, the velocity of the solid-liquid interface, and heat transfer characteristics are investigated.

1. Introduction

Interest in utilizing clean energy is growing because of environmental considerations. Solar energy is one of the promising clean energies, but due to its periodic feature, a heat storage device is needed. The thermal energy storage system using a Phase Change Material (PCM) is an attractive method because a large amount of latent heat can be stored or released during the melting or solidification process of the PCM. Variety of phase change materials is used in the thermal energy storage device so as to increase its heat storage capacity and reduce the temperature difference during operation. In the thermal energy storage process, the hot working fluid from the solar energy collector flows into the thermal energy storage device to melt the PCM and store thermal energy in the form of latent heat. Natural convection plays a significant role in melting due to the temperature difference in the liquid phase.

Natural convection controlled melting in a rectangular cavity under the boundary condition of the first and second kinds has been investigated extensively (Ho and Viskanta, 1984; Gadgil and Gobin, 1984; Bejan, 1989; Zhang and Bejan, 1989; Zhang and Chen, 1994). In a solar energy utilization system, the working fluid absorbs heat in the solar energy collector and transfers the heat to the latent heat thermal energy storage system via convection (Zhang and Faghri, 1995; 1996; Zhang et al., 1997). Therefore, melting in the latent heat thermal energy storage system is neither under boundary conditions of the first kind nor under boundary condition of the second kind. It is under the boundary conditions of the third kind. In order to thoroughly understand the mechanism in the latent heat thermal energy storage unit, it is necessary to study melting in an enclosure under the boundary of the third kind.

2. Physical Model

The physical model under consideration is shown in Fig. 1. The enclosure with height of H and width of L is filled with PCM at its melting point, T_m. The top, bottom and the left side of the enclosure are adiabatic. At time $t>0$, the right side of the

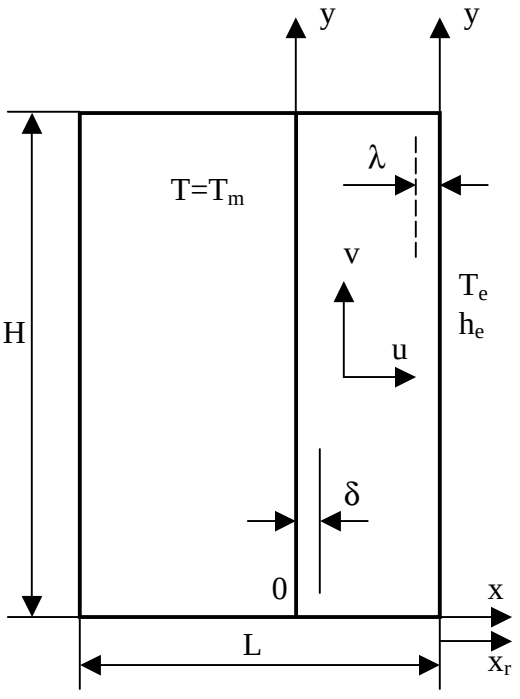

Fig. 1 Physical model

enclosure is in contact with working fluid at temperature of T_e. The convective heat transfer coefficient between the working fluid and the right wall is h_e and it is a constant. It is assumed the thickness of the right sidewall is very small and therefore, the conduction thermal resistance of the wall is negligible. The melting process can be divided into two stages: conduction and convection stages. During the conduction stage, conduction is the dominant model of heat transfer. The problem can be simplified as a 1-D melting problem under boundary condition of the third kind and the analytical solution is available (Cho and Sunderland, 1981). The melting process enters the convection stage when the thickness of the melting layer increases and natural convection becomes the dominant mode of heat transfer. Although the process is still unsteady, the transient terms in mathematical equations describing in the melting process will have negligible effect and the process is considered to be quasi-steady (Bejan, 1989).

When the melting is in the early stage of the convection regime, the solid-liquid interface can be assumed to be sufficiently straight and vertical. In addition, the following assumptions are made:

1. The properties of liquid PCM are constants except for density, which is a function of temperature (Boussinesq assumption). The liquid is Newtonian and incompressible.
2. The Prandtl number of the liquid phase change material is greater much than 1. This assumption is valid for most PCMs (Zhang and Bejan, 1989).
3. The liquid motion induced by volumetric variation during melting is neglected, i.e., the density of the solid is equal to that of the liquid.

The liquid phase can be divided into three regions: (1) cold boundary layer near solid-liquid interface, (2) warm boundary layer near the heated vertical wall, and (3) the core region between these two boundary layers (Bejan, 1989). The governing equations for the three regions are described below.

2.1 The cold boundary layer

The analysis of the cold boundary layer is performed in a frame (x-y system) that is attached onto the solid-liquid interface. Since the Prandtl number of the liquid is much larger than unity, the inertia terms in the momentum equation can be neglected. The advection induced by the solid- liquid interface motion in the boundary layer equations can also be neglected since the solid- liquid interface velocity is typically several orders of magnitude smaller than the natural convective velocity in the boundary layer (Gadgil and Gobin 1984). The momentum and energy equations for the cold boundary layer are

$$\frac{\partial^3 v}{\partial x^3} + \frac{g\beta}{\nu}\frac{\partial T}{\partial x} = 0 \tag{1}$$

$$u\frac{\partial T}{\partial x} + v\frac{\partial T}{\partial y} = \alpha\frac{\partial^2 T}{\partial x^2} \tag{2}$$

These equations were solved by an integral method. By following the procedure similar to Bejan (1989) and Zhang and Bejan (1989), an ordinary differential equation about could boundary layer thickness, δ, is obtained

$$\frac{2k(T_c - T_m)^2}{\rho h_m \delta} + \frac{g\beta(T_c - T_m)}{36\nu}\frac{d}{dy}\left[\delta^3(T_c - T_m)\right] - \frac{g\beta}{60\nu}\frac{d}{dy}\left[\delta^3(T_c - T_m)^2\right] = -2\alpha\frac{T_c - T_m}{\delta} \tag{3}$$

where T_c is the core temperature, ρ is density, h_m is latent heat of melting, β is the thermal expansion coefficient, ν and α are kinematic viscosity and thermal diffusivity respectively.

Since the cold boundary layer starts from the top of the enclosure, the boundary condition of eq. (3) is

$$\delta(H) = 0 \tag{4}$$

The solid-liquid interface velocity, u_0, can be obtained by energy balance at the interface. Considering the assumed temperature profile in the cold boundary layer used in the integral solution, the solid-liquid interface velocity is

$$u_0 = \frac{2k(T_c - T_m)}{\rho h_m \delta} \tag{5}$$

2.2 The warm boundary layer

The warm boundary layer is attached onto the heated wall, i.e., on a stationary frame (x_r-y). The Analysis of the warm boundary layer is very similar to that of the cold boundary layer. The momentum and the energy equations are the same as eqs. (1-2) except the (x, v, T) are replaced with (x_r, v_r, T_r). After performing the integral solution, the equation of the warm boundary layer thickness becomes

$$\frac{g\beta}{90\nu}\frac{d}{dy}\left[\lambda^3 (T_w - T_c)^2\right] + \frac{g\beta (T_w - T_c)\lambda^3}{36\nu}\frac{dT_c}{dy} = -2\alpha \frac{T_w - T_c}{\lambda} \tag{6}$$

The boundary condition of eq. (6) is

$$\lambda(0) = 0 \tag{7}$$

The wall temperature, T_w, can be obtained by considering energy balance at the right side wall of the enclosure

$$\frac{2k(T_w - T_c)}{\lambda} = h_e (T_e - T_w) \tag{8}$$

2.3 The core region

The temperature of the core region, T_c, can be obtained by considering the fact that the horizontal entrainment velocities of the two boundary layers represent the same core flow (Bejan, 1989; Zhang and Bejan, 1989).

$$\delta^3 (T_c - T_m) = \lambda^3 (T_w - T_c) \tag{9}$$

The core temperature is the lowest at the bottom and highest at the top of the enclosure, i.e.,

$$T_c(0) = T_m \tag{10}$$

$$T_c(H) = T_w(H) \tag{11}$$

3. Solutions

Defining the following dimensionless variables

$$Ste = \frac{c_p (T_e - T_m)}{h_m} \qquad Ra_* = \frac{g\beta (T_e - T_m) H^3}{\nu\alpha} \qquad Y = \frac{y}{H} \qquad \Delta = \frac{\delta}{H} Ra_*^{\frac{1}{4}}$$

$$\Lambda = \frac{\lambda}{H} Ra_*^{\frac{1}{4}} \qquad \theta = \frac{T - T_m}{T_e - T_m} \qquad Ra = \overline{\theta_w} Ra_* \qquad Bi = \frac{h_e H}{k} \qquad U_0 = \frac{u_0 H \rho h_m}{k(T_e - T_m) Ra_*^{1/4}} \tag{12}$$

the following dimensionless equations are obtained

$$2Ste\frac{\theta_c^2}{\Delta} + \frac{\theta_c}{36}\frac{d}{dY}(\Delta^3 \theta_c) - \frac{1}{60}\frac{d}{dY}(\Delta^3 \theta^2{}_c) = -\frac{2\theta_c}{\Delta} \tag{13}$$

$$\frac{1}{90}\frac{d}{dY}\left[\Lambda^3 (\theta_w - \theta_c)^2\right] + \frac{\Lambda^3 (\theta_w - \theta_c)}{36}\frac{d\theta_c}{dY} = -\frac{2(\theta_w - \theta_c)}{\Lambda} \tag{14}$$

$$\Delta^3\theta_c = \Lambda^3(\theta_w - \theta_c) \tag{15}$$

$$\frac{2(\theta_w - \theta_c)}{\Lambda} = BiRa_*^{-1/4}(1-\theta_w) \tag{16}$$

and their corresponding boundary conditions are

$$Y = 0 \qquad \Lambda = 0 \qquad \theta_c = 0 \tag{18}$$

$$Y = 1 \qquad \Delta = 0 \qquad \theta_c = \theta_w \tag{19}$$

The dimensionless solid-liquid interface velocity is

$$U_0 = 2\theta_c / \Delta \tag{20}$$

The set of ordinary differential equations (13-14), with boundary conditions specified by eq. (18-19) is a boundary value problem. The boundary value problem was solved by using a shooting method in the interval of Y=0 and Y=1. The objective of the shooting method was to satisfy boundary condition $\Delta(1)=0$ by properly adjusting $\Delta(0)$. Equations (13-14) are discretized using an implicit scheme. The discretized equations and eqs. (15-16) are solved using an iteration method. Double procession was employed in all calculations to ensure the accuracy. After the grid size independent test, the number of nodal points along the height is chosen to be N=2000, which corresponds to a grid size of $\Delta Y=0.0005$. In the iterative solution procedure, the converged solution for a particular Y is obtained when the difference between two consecutive iteration for all four variables are less than 10^{-9}. The converged solution for the entire problem is obtained when shooting error for $\Delta(1)$ is less than 10^{-9}.

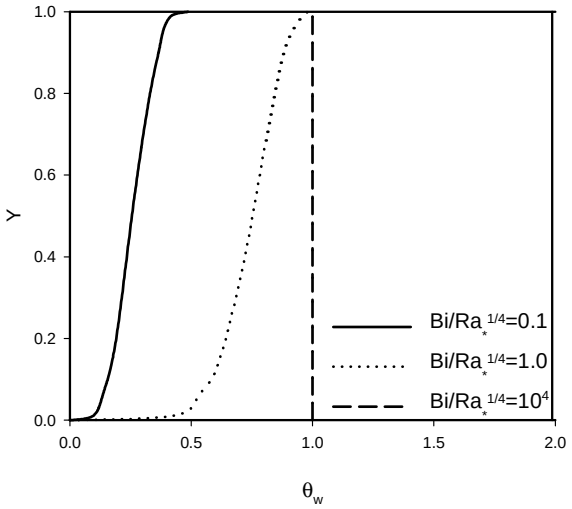

Fig. 2 Dimensionless wall temperature

4. Results and Discussions

Figure 2 shows the distribution of the dimensionless wall temperature at different external convective heat transfer conditions. The Stefan number is usually very small for the solid-liquid phase change system, and it has negligible effect on the results (Bejan, 1989). Therefore, the results in Fig. 2 are obtained for the case of Ste=0. It can be seen that the dimensionless wall temperature is a constant when $Bi/Ra_*^{1/4}=10^4$, which agree with the case of the boundary condition of the first kind ($T_w=T_e$). The dimensionless wall temperature increases with increasing Y for lower $Bi/Ra_*^{1/4}$. The wall temperature increases rapidly near Y=0 and Y=1, and it is linear function of Y in the middle portion along the height direction. When $Bi/Ra_*^{1/4}=0.1$, the result is similar to that of constant heat flux heating in Zhang and Bejan (1989).

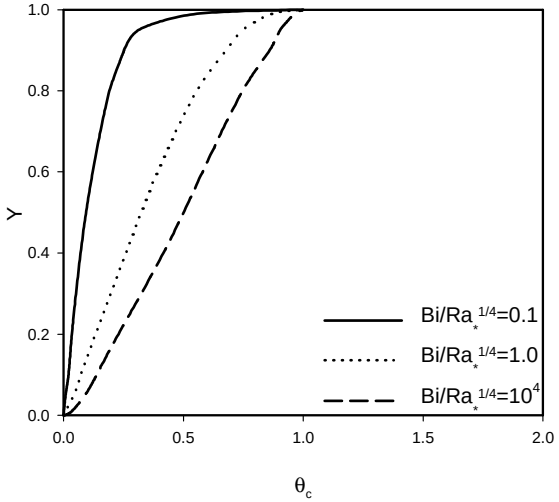

Fig. 3 Dimensionless core temperature

The distributions of the core temperature are shown in Fig. 3. It can be seen that the core temperature is linear function of Y when $Bi/Ra_*^{1/4}=10^4$, which is similar to the case of

constant temperature heating. The core temperature decreases when $Bi/Ra_*^{1/4}$ decreases because the amount of heat absorbed by the PCM is lower for smaller $Bi/Ra_*^{1/4}$. When $Bi/Ra_*^{1/4}=0.1$, the distribution of the core temperature is similar to that of constant heat flux heating in Zhang and Bejan (1989). The results in Fig. 2 and 3 indicated that the present model is capable to simulate melting in an enclosure subjected all three kinds of boundary conditions.

The variation of the dimensionless solid-liquid interface velocity along Y direction for different external heat transfer conditions are shown in Fig. 4. For the case of $Bi/Ra_*^{1/4}=10^4$, the present results agreed very well with the results of Bejan (1989), who investigated melting in an enclosure under the boundary conditions of the first kind. As can be seen from Fig. 4, the solid-liquid interface velocity decreases with decreasing $Bi/Ra_*^{1/4}$ since the heat absorbed by the PCM decreases with decreasing $Bi/Ra_*^{1/4}$. The heat transfer characteristics and the rate of melting are shown in Fig. 5. The heat transfer characteristics is evaluated by using the following parameter

$$\frac{Nu}{Ra_*^{1/4}} = \frac{2(\theta_w - \theta_c)}{\Lambda \theta_w} \qquad (21)$$

where, Nu=hL/k is Nusselt number. It should be pointed out that the temperature difference in Ra_* is (T_e-T_m), which is really not the driving force of natural convection. The driving force for natural convection in the liquid phase should be (T_w-T_m). Therefore, the Rayleigh number based on (T_w-T_m), Ra, is defined and its relationship with Ra_* is shown in eq. (9). Substituting eq. (9) into eq. (21), the following parameter is obtained and it is a parameter that can accurately reflect the characteristics of the natural convection.

$$\frac{Nu}{Ra^{1/4}} = \frac{2(\theta_w - \theta_c)}{\Lambda \theta_w \overline{\theta_w}^{1/4}} \qquad (22)$$

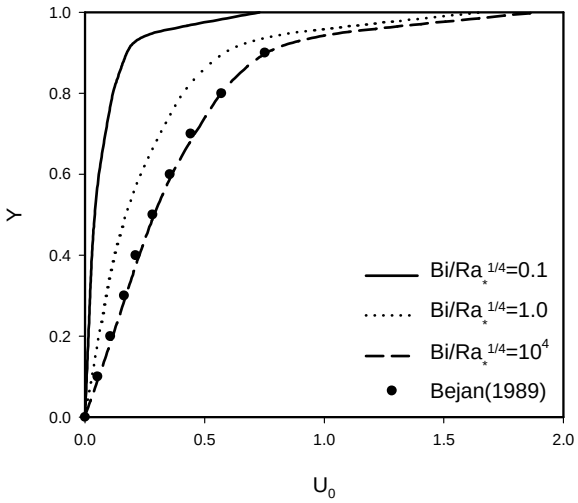

Fig. 4 Solid-liquid interface velocity

It can be seen from Fig. 5 that the difference between the parameters defined by eqs. (21) and (22) vanishes and they become a constant equal to 0.374 when $Bi/Ra_*^{1/4}>10^2$, which are same as the case of constant temperature heating in Bejan (1989). Therefore, the melting problem can be treated as boundary condition of the first kind when $Bi/Ra_*^{1/4}>10^2$. $Nu/Ra^{1/4}$ increases with decreasing $Bi/Ra_*^{1/4}$ and its value approaches the results of constant heat flux heating when $Bi/Ra_*^{1/4}=0.1$.

The melting rate can be obtained by

$$R = \frac{V/V_0}{SteFo}\frac{L}{H} = \int_0^1 U_0(Y)dY \qquad (23)$$

where, V/V_0 is the ratio of the liquid volume over the total volume of the enclosure. As can be seen from Fig. 5, the rate of melting is same as that of boundary condition of the first kind when $Bi/Ra_*^{1/4}>10^2$. The rate of melting decreases with decreasing $Bi/Ra_*^{1/4}$ since the wall temperature decreases with decreasing $Bi/Ra_*^{1/4}$.

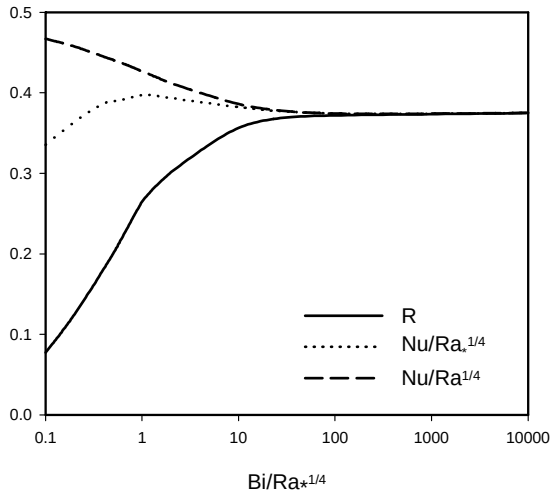

Fig. 5 Heat transfer and melting rate

5. Conclusion

Natural convection controlled melting in an enclosure under boundary condition of the third kind is investigated analytically. The results show that the melting process is similar to that under boundary condition of the first kind when $Bi/Ra_*^{1/4}>10^2$. The results approach to that under boundary condition of the second kind when $Bi/Ra_*^{1/4}$ decreases. Therefore, the present model provided a generalized solution for natural convection controlled melting in an enclosure and it is applicable to all three kinds of boundary conditions. The heat transfer and melting rate under different condition can be calculated by using Fig. 5.

References

A. Bejan, Analysis of Melting by Natural Convection in an Enclosure, Int. J. Heat and Fluid Flow, Vol. 10, pp. 245-252, 1989

S. H. Cho and J.E. Sunderland, Approximate Temperature Distribution for Phase change of semi-Infinite Body, ASME J. Heat transfer, Vol. 103, pp. 401-403, 1981

A. Gadgil and D. Gobin, Analysis of Two Dimensional Melting in Rectangular Enclosures in Presence of Convection, AMSE J. Heat Transfer, Vol. 106, pp. 20-26, 1984

C.J. Ho and Viskanta, Heat Transfer During Melting from an Isothermal Vertical Wall, ASME J. Heat Transfer, Vol. 106, pp. 12-19, 1984.

Y. Zhang and Z.Q. Chen, Effect of Wall Conduction on Melting in an Enclosure Heated by Constant Rate, Int. J. Heat Mass Transfer, Vol. 37, No. 2, pp. 340-343, 1994.

Y. Zhang, Z.Q. Chen and A. Faghri, Heat Transfer During Solidification around a Horizontal Tube with Internal Convective Cooling, ASME J. Solar Energy Engineering, Vol. 119, No. 1, pp. 44-47, 1997.

Y. Zhang and A. Faghri, Analysis of Thermal Energy Storage System with Conjugate Turbulent Forced Convection, AIAA J. Thermophysics and Heat Transfer, Vol. 9, No. 4, pp. 722-726, 1995.

Y. Zhang and A. Faghri, Semi- Analytical Solution of Thermal Energy Storage System with Conjugate Laminar Forced Convection, Int. J. Heat Mass Transfer, Vol. 39, No. 4, pp. 717-724, 1996.

Z. Zhang and A. Bejan, Melting in an Enclosure Heated at Constant Rate, Int. J. Heat Mass Transfer, Vol. 32, pp. 1063-1076, 1989.